

# THE PERFORMANCE OF VARIOUS ARTIFICIAL NEURONS INTERCONNECTIONS IN THE MODELLING AND EXPERIMENTAL MANUFACTURING OF THE COMPOSITES

## PREDSTAVITEV RAZLIČNIH UMETNIH NEVRONSKIH POVEZAV PRI MODELIRANJU IN EKSPERIMENTALNI IZDELAVI KOMPOZITOV

**Mohsen Ostad Shabani, Ali Mazahery**

Karaj Branch, Islamic Azad University, Karaj, Iran  
vahid\_ostadshabany@yahoo.com

*Prejem rokopisa – received: 2011-05-31; sprejem za objavo – accepted for publication: 2011-07-06*

This study reports the performance of different artificial neural network (ANN) training algorithms in the prediction of mechanical properties. First, an experimental investigation was carried out on the mechanical behavior of an A356 composite reinforced with B<sub>4</sub>C particulates and then an ANN modeling was implemented in order to predict the mechanical properties, including the yield stress, UTS, hardness and elongation percentage. After the preparation of the training set, the neural network was trained using different training algorithms, hidden layers and the number of neurons in hidden layers. The test set was used to check the system accuracy for each training algorithm at the end of the learning. The results show that the Levenberg-Marquardt learning algorithm gave the best prediction for the yield stress, UTS, hardness and elongation percentage of the A356 composite reinforced with B<sub>4</sub>C particulates.

Keywords: composite, hardness, mechanical properties, ANN

V tem delu smo najprej opredelili mehanske lastnosti, vključno z mejo plastičnosti, natezno trdnostjo, trdoto in raztežkom kompozita A356, ojačenega z delci B<sub>4</sub>C, in nato uporabili kombinacijo umetne nevronske mreže in metode končnih elementov. Po pripravi treningpostavitve je bila nevronska mreža preizkušena z uporabo različnih algoritmov, skritih plasti in števila nevronov v skritih plasteh. Treningpostavitev je bila uporabljena za preverjanje natančnosti za vsak algoritem na koncu učenja. Rezultati kažejo, da da Levenberg-Marquardtov učni logaritem najboljšo napoved meje plastičnosti, natezne trdnosti, trdote in raztežka za kompozit A356, ki je ojačen z delci B<sub>4</sub>C.

Ključne besede: kompozit, trdota, mehanske lastnosti, ANN

## 1 INTRODUCTION

Large quantities of castings are made each year from the aluminium alloy A356 (also known as Al-7Si-0.3Mg). This alloy is one of the most popular alloys used in industry due to its high fluidity and good "castability"<sup>1-5</sup>.

The addition of hard particles to a ductile metal matrix produces a material whose mechanical properties are intermediate between the matrix alloy and the ceramic reinforcement. The casting cooling rate, the reinforcement volume fraction, size, shape, and spatial distribution are the most important parameters, playing a role in the enhancement of the composite's mechanical properties. A stronger adhesion at the particle/matrix interface improves the load transfer, increasing the yield strength and stiffness, and delays the onset of particle/matrix de-cohesion<sup>6</sup>.

An ANN is a logical structure with multi-processing elements, which are connected through interconnection weights. The knowledge is represented by the interconnection weights, which are adjusted during the learning phase. This technique is especially valuable in

processes where a complete understanding of the physical mechanisms is very difficult, or even impossible to acquire, as in the case of material properties where no satisfactory analytical model exists<sup>7-14</sup>.

The aim of this study was to investigate the prediction performance of various training algorithms using a neural network computer program for the mechanical properties of the A356 composite reinforced with B<sub>4</sub>C particulates. The results showed that the Levenberg-Marquardt learning algorithms gave the best result for this study.

## 2 EXPERIMENTAL

In this study, A356 was used as the matrix material and different volume fractions of B<sub>4</sub>C particles (1 % to 15 % B<sub>4</sub>C) with particle sizes ranging from 1 μm to 5 μm were used as the reinforcements.

The melt-particle slurry was produced by a mechanical stirrer. Approximately 5 kg of A356 alloy was charged into the graphite crucible and heated up to a temperature above the alloy's melting point (750 °C). The graphite stirrer, fixed on the mandrel of the drilling

machine, was introduced into the melt and positioned just below the surface of the melt. It was stirred at approximately 600 r/min and 750 °C. Then the step casting was poured into the CO<sub>2</sub>-sand mould.

Microscopic examinations of the composites and matrix alloy were carried out using an optical microscope. The porosity measurements of the composites were obtained using Archimedes's method. Hardness and tensile tests were used to assess the mechanical behavior of the composites and the matrix alloy.

### 2.1 Prediction of cooling rate and temperature gradient with EEM

The numerical model is applied to simulate the solidification of binary alloys; the mathematical formulation of this solidification problem is given<sup>15</sup>:

$$\rho C \frac{\partial T(x, y, z, t)}{\partial t} = K \nabla^2 T(x, y, z, t) + q \quad (1)$$

where  $\rho$ /(kg/m<sup>3</sup>) is the density,  $K$ /(W/(m K)) is the thermal conductivity,  $C$ /(J/(kg K)) is the specific heat,  $q$ /(W/m<sup>3</sup>) is the rate of energy generation,  $T$ /K is the temperature, and  $t$ /s is the time.

The release of latent heat between the liquidus and solidus temperatures is expressed by:

$$q = \rho L \frac{\delta f_s}{\delta t} \quad (2)$$

where  $L$ /(J/kg) is the latent heat and  $f_s$  is the local solid fraction.

The fraction of solid in the mushy zone is estimated by the Scheil equation, which assumes perfect mixing in the liquid and no solid diffusion. With the liquidus and solidus having constant slopes,  $f_s$  is then expressed as:

$$f_s = 1 - \left( \frac{T_f - T}{T_f - T_{liq}} \right)^{1/(k_0 - 1)} \quad (3)$$

where  $T_f$ /K is the melting temperature,  $T_{Liq}$ /K is the liquidus temperature and  $k_0$  is the partition coefficient. Then<sup>15</sup>:

$$\frac{\delta f_s}{\delta t} = \frac{1}{(k_0 - 1)(T_f - T_{liq})} \left( \frac{T_f - T}{T_f - T_{liq}} \right)^{(2 - k_0)/(k_0 - 1)} \frac{\delta T}{\delta t} \quad (4)$$

The latent heat released during the solidification of the remaining liquid of eutectic composition was taken into account by a device that considers a temperature accumulation factor.

$$\rho C' \frac{\partial T(x, y, z, t)}{\partial t} = K \nabla^2 T(x, y, z, t) + q \quad (5)$$

where  $C'$  can be considered as a pseudo-specific heat given by:

$$C' = C_M - L \frac{\delta f_s}{\delta T} \quad (6)$$

$$C_M = (1 - f_s)C_L + f_s C_s \quad (7)$$

where the subscripts L, S and M refer to liquid, solid and mushy, respectively. The other properties, such as the thermal conductivity and the density in the mushy zone, are described in a similar way to the specific heat:

$$K_M = (1 - f_s)K_L + f_s K_s \quad (8)$$

$$\rho_M = (1 - f_s)\rho_L + f_s \rho_s \quad (9)$$

The finite-element method (FEM) was used for discretization. Based on the above transient-temperature model, the FEM method is used to calculate the transient temperature, cooling rate and temperature gradient (G).

### 2.2 Neural network training algorithms

There are various training algorithms used in neural network applications. However, it is difficult to predict which of these will be the fastest one for any problem. Generally, it depends on some factors: the structure of the networks, in other words, the number of hidden layers, weights and biases in the network, aimed error during the learning, and application area, for instance, pattern recognition or classification or the function approximation problem. However, the data structure and the uniformity of the training set are also important factors that affect the system accuracy and performance. Some of the famous training algorithms are as follows<sup>7-14,16-26</sup>:

Resilient back propagation ( $R_{prop}$ ): is a network training function that updates weight and bias values according to the  $R_{prop}$  algorithm.

Random order incremental training with learning functions: trains a network with weight and bias learning rules using incremental updates after each presentation of an input. Inputs are presented in a random order.

Gradient descent back propagation: is a network training function that updates weight and bias values according to the gradient descent.

BFGS quasi-Newton back propagation: is a network training function that updates weight and bias values according to the BFGS quasi-Newton method.

Bayesian regularization: is a network training function that updates the weight and bias values according to LM optimization. It minimizes a combination of squared errors and weights, and then determines the correct combination so as to produce a network that generalizes well. The process is called Bayesian regularization.

In the analysis of the performance of various training algorithms, the same prepared learning and test set were used in the training processes of each learning algorithm. The performance analyses were made from the viewpoint of training duration, error minimization and prediction achievement. The neural network predictions were directly compared with the experimentally obtained data to evaluate the learning performance. The mean square error (MSE), which is a statistical and scientific

error-computation method, was used to analyze the error<sup>25</sup>.

### 3 RESULTS AND DISCUSSION

Microscopic examinations were carried out on the metal-matrix composite. **Figure 1** shows that the B<sub>4</sub>C particles were distributed between the dendrite branches and were frequently clustered together, leaving the dendrite branches as particle-free regions in the material.

**Figure 2** shows the variation of porosity with B<sub>4</sub>C content. It indicates that an increasing amount of porosity is observed with increasing the volume fraction

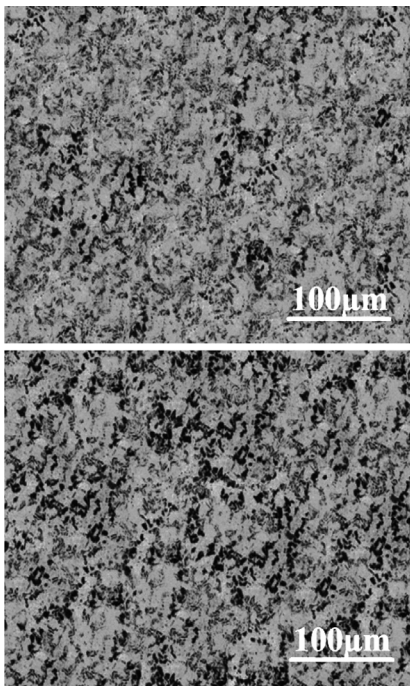


**Figure 1:** Typical optical micrographs: a) the composite with the volume fraction of B<sub>4</sub>C 4 %, b) the composite with 13 % B<sub>4</sub>C

**Slika 1:** Tipičen optični posnetek: a) kompozit z volumenskim deležem B<sub>4</sub>C 2 %, b) kompozit s 15 % B<sub>4</sub>C

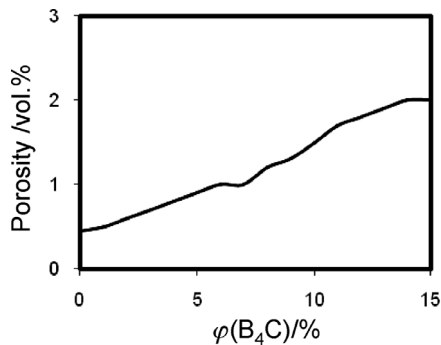


**Figure 2:** Variations of porosity as a function of the volume fraction of B<sub>4</sub>C

**Slika 2:** Spremembe poroznosti v odvisnosti od volumenskega deleža B<sub>4</sub>C

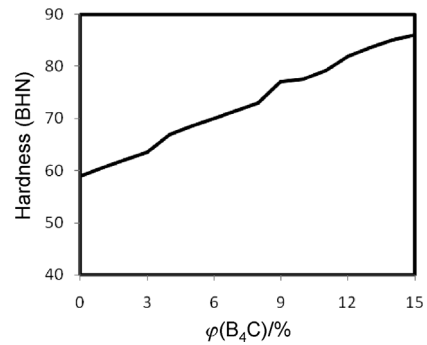


**Figure 3:** Variations of the hardness value of the samples as a function of the volume fraction of B<sub>4</sub>C

**Slika 3:** Spremembe trdote vzorcev v odvisnosti od volumenskega deleža B<sub>4</sub>C

of the composites. The porosity level increased, since the contact surface area was increased<sup>27-31</sup>.

**Figure 3** displays the results of the hardness tests. The hardness of the MMCs increases with the volume fraction of particulates in the alloy matrix. The higher hardness of the composites could be attributed to the fact that the B<sub>4</sub>C particles act as obstacles to the motion of dislocations<sup>32-36</sup>. **Figure 4** shows the typical stress-strain curves obtained from uniaxial tension tests. The considerable increase in strain-hardening observed during the plastic deformation of composites is rationalized by the resistance of the hard reinforcing particles to the slip behavior of the Al matrix. The elongation to fracture of the composite materials was found to be very low, and no necking phenomenon was observed before fracture. On the other hand, the elongation to fracture of the un-reinforced Al alloy was about 15 %.

The input and output data set of the model is illustrated schematically in **Figure 5**. In **Figure 6**, the obtained MSE values for training data were given for each training algorithm. The obtained error values for

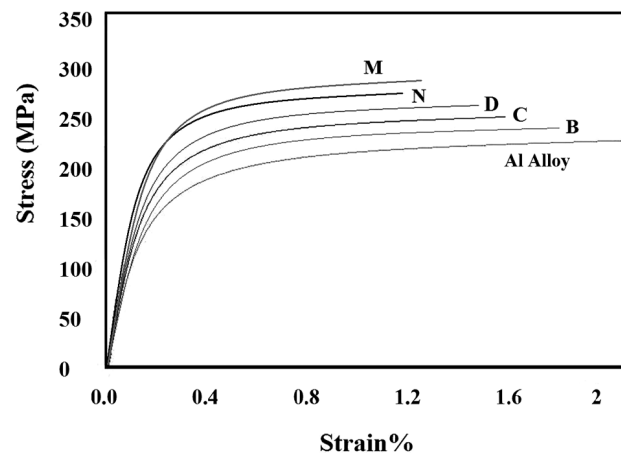


**Figure 4:** Stress-strain curves for volume fractions Al/ 3 % B<sub>4</sub>C (B), Al/ 7 % B<sub>4</sub>C (C), Al/ 10 % B<sub>4</sub>C (D), Al/ 12 % B<sub>4</sub>C (M) and Al/ 15 % B<sub>4</sub>C (N)

**Slika 4:** Odvisnosti napetost – deformacija za volumenske deleže Al/ 3 % B<sub>4</sub>C (B), Al/ 7 % B<sub>4</sub>C (C), Al/ 10 % B<sub>4</sub>C (D), Al/ 12 % B<sub>4</sub>C (M) in Al/ 15 % B<sub>4</sub>C (N)

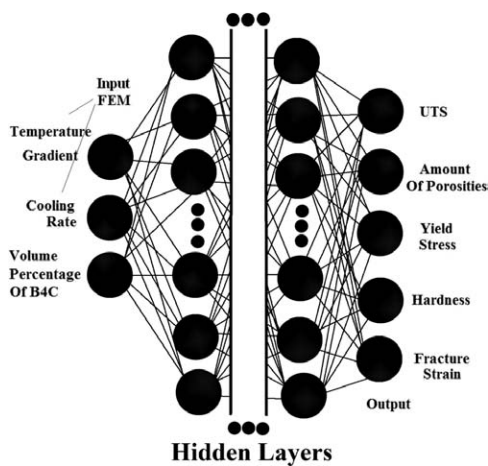
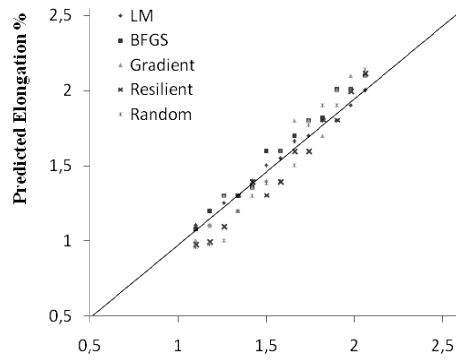
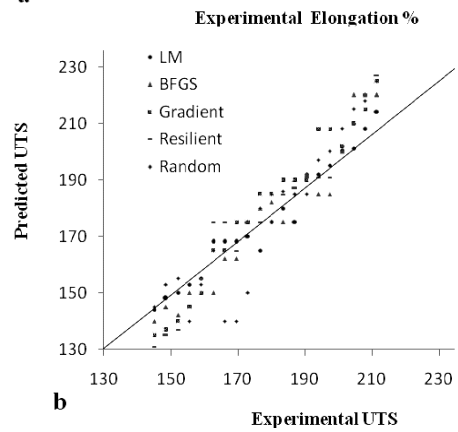


Figure 5: Schematic representation of the neural network architecture  
 Slika 5: Shematičen prikaz nevronske arhitekture

different numbers of neurons in the hidden layers and the number of hidden layers were analyzed and presented graphically. This figure also gives information about the accuracy of five famous training algorithms depending on the number of neurons in the hidden layers and the number of hidden layers. It is evident from this figure that the smallest error value was obtained by using the Levenberg-Marquardt training algorithm with two hidden layers and eight neurons ( $MSE = 6.4$ ). BFGS quasi-Newton back propagation with three hidden layers and nine neurons in the hidden layers follows the



a



b

Figure 7: Comparison between the experimental and predicted values: a) elongation percentage, b) UTS

Slika 7: Primerjava med eksperimentalnimi in predvidenimi vrednostmi za: a) raztezek in b) natezno trdnost

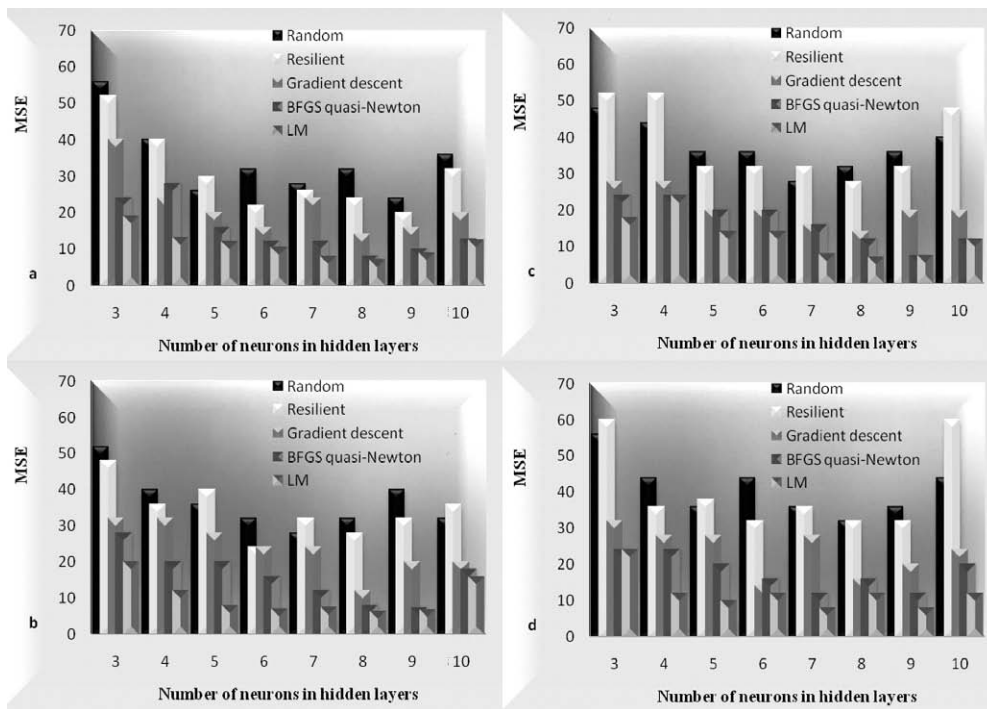


Figure 6: Evaluation of the training performance of the networks for different training algorithms according to the  $MSE$  values with: a) one hidden layer, b) two hidden layers, c) three hidden layers and d) four hidden layers

Slika 6: Ocena parametrov treninga mreže za različne treningalgoritme po  $MSE$ -vrednostih za: a) eno skrito plast, b) dve skrite plasti, c) tri skrite plasti in d) štiri skrite plasti

Levenberg-Marquardt algorithm ( $MSE = 8.1$ ), and thirdly the gradient descent back propagation including four hidden layers and six neurons in the hidden layers has clearly much more error than the previous two cases ( $MSE = 14.4$ ). The most error was obtained from the Resilient back-propagation training algorithm and the Random order incremental training with learning functions. The Levenberg-Marquardt training algorithm was found to be the fastest training algorithm; however, it requires more memory with the same error convergence bound compared to the training methods<sup>25</sup>.  $MSE$  is a good criterion to have information about learning performance. The iterations were continued until it is decided that the minimum  $MSE$  error is obtained.

**Figure 7** shows the efficacy of the optimization scheme by comparing the ANN results with the experimental values. There is a convincing agreement between the experimental values and the predicted values for UTS and the elongation percentage of the A356 composite reinforced with  $B_4C$  particulates for the Levenberg-Marquardt training algorithm.

#### 4 CONCLUSION

- 1) The mechanical properties modeling was developed to predict the hardness, yield stress, ultimate tensile strength and elongation percentage.
- 2) The effect of various training algorithms on the prediction of the mechanical properties of the fabricated A356 composite reinforced with  $B_4C$  particulates was investigated. The prediction of the ANN model was found to be in good agreement with the experimental data.
- 3) According to the results, the Levenberg-Marquardt learning algorithm gave the best prediction for hardness, yield stress, ultimate tensile strength and elongation percentage for the A356 composite. It is believed that an ANN with two hidden layers and eight neurons ( $MSE = 6.4$ ) gave an accurate prediction of the mechanical properties of the fabricated A356 composite reinforced with  $B_4C$  particulates.

#### 5 REFERENCES

- <sup>1</sup> A. Mazahery, M. O. Shabani, J. Mater. Eng. Perform., 21 (2012), 247–252
- <sup>2</sup> H. Möller, G. Govender, W. E. Stumpf, Trans. Nonferrous Met. Soc. China, 20 (2010), 1780–1785
- <sup>3</sup> L. Ceschini, A. Morri, G. Sambogna, Journal of Materials Processing Technology, 204 (2008), 231–238
- <sup>4</sup> M. O. Shabani, A. Mazahery, A. Bahmani, P. Davami, N. Varahram, Kovove Mater, 49 (2011) 4, 253–258
- <sup>5</sup> N. Chomsaeng, M. Haruta, T. Chairuangri, H. Kurata, S. Isoda, M. Shiojiri, Journal of Alloys and Compounds, 496 (2010), 478–487
- <sup>6</sup> A. Evans, C. S. Marchi, A. Mortensen, Kluwer Academic Publishers, Dordrecht, Netherlands, 2003
- <sup>7</sup> S. K. Singh, K. Mahesh, A. K. Gupta, Materials and Design, 31 (2010), 2288–2295
- <sup>8</sup> F. Karimzadeh, A. Ebnonnasir A. Foroughi, Materials Science and Engineering A, 432 (2006), 184–190
- <sup>9</sup> N. Altinkok, R. Koker, Materials and Design, 25 (2004), 595–602
- <sup>10</sup> A. M. Hassan, A. Alrashdan, M. T. Hayajneh, A. T. Mayyas, Journal of Materials Processing Technology, 209 (2009), 894–899
- <sup>11</sup> M. Ohlsson, Artificial Intelligence in Medicine, 30 (2004), 49–60
- <sup>12</sup> S. K. Singh, K. Mahesh, A. K. Gupta, Materials and Design, 31 (2010), 2288–2295
- <sup>13</sup> P. J. Lisboa, A. F. G. Taktak, A systematic review, Neural Networks, 19 (2006), 408–415
- <sup>14</sup> A. M. Rashidi, A. R. Eivani, A. Amadeh, Computational Materials Science, 45 (2009), 499–504
- <sup>15</sup> M. O. Shabani, A. Mazahery, Int. J. of Appl. Math and Mech, 7 (2011), 89–97
- <sup>16</sup> A. Mazahery, M. O. Shabani, Powder Technology, 217 (2012), 558–565
- <sup>17</sup> R. Koker, N. Altinkok, A. Demir, Materials and Design, 28 (2007), 616–627
- <sup>18</sup> M. O. Shabani, A. Mazahery, Applied Mathematical Modelling, 35 (2011), 5707–5713
- <sup>19</sup> L. Fratini, G. Buffa, D. Palmeri, Computers and Structures, 87 (2009), 1166–1174
- <sup>20</sup> R. Hamzaoui, M. Cherigui, S. Guessasm, O. ElKedim, N. Fenineche, Materials Science and Engineering B, 163 (2009), 17–21
- <sup>21</sup> N. S. Reddy, A. K. Prasada Rao, M. Chakraborty, B. S. Murty, Materials Science and Engineering A, 391 (2005), 131–140
- <sup>22</sup> Z. Sterjovski, D. Nolan, K. R. Carpenter, D. P. Dunne, J. Norrish, Journal of Materials Processing Technology, 170 (2005), 536–544
- <sup>23</sup> S. H. Mousavi Anijdan, A. Bahrami, H. R. Madaah Hosseini, A. Shafyei, Materials and Design, 27 (2006), 605–609
- <sup>24</sup> M. O. Shabani, A. Mazahery, Synthetic Metals, 161 (2011), 1226–1231
- <sup>25</sup> R. Koker, N. Altinkok, A. Demir, Materials and Design, 28 (2007), 616–627
- <sup>26</sup> M. Tatlier, H. K. Cigizoglu, A. Erdem-Şenatalar, Computers and Chemical Engineering, 30 (2005), 137–146
- <sup>27</sup> M. Zamzam, D. Ros, J. Grosch, Key Eng Mater, 79–80 (1993), 235–246
- <sup>28</sup> M. Kok, Ph. D. Thesis, The Institute of Science and Technology of Elazig University, Turkey, 1999
- <sup>29</sup> W. Zhou, Z. M. Xu, Casting of SiC reinforced metal matrix composites, J. Mater. Process. Technol., 63 (1997), 358–363
- <sup>30</sup> S. Ray, Porosity in foundry composites prepared by vortex method, in: S. G. Fishman, A. K. Dhingra (Eds.), ASM/TMS, 1988, 77–80
- <sup>31</sup> D. J. Lloyd, B. Chamberian, ASM, Illinois, 1988, 263–269
- <sup>32</sup> F. M. Hosking, F. Folgar Portillo, R. Wunderlin, R. Mehrabian, Composites of aluminium alloys: fabrication and wear behaviour, J. Mater. Sci., 17 (1982), 477–498
- <sup>33</sup> M. Roy, B. Venkataraman, V. V. Bhanuprasad, Y. R. Mahajan, G. Sundararajan, Metall. Trans. A, 23 (1992), 2833–2846
- <sup>34</sup> S. Chung, B. H. Hwang, Tribol. Int., 27 (1994) 5, 307–314
- <sup>35</sup> S. Skolianos, T. Z. Kattamis, Mater. Sci. Eng. A, 163 (1993), 107–113
- <sup>36</sup> P. N. Bindumadhavan, H. K. Wah, O. Prabhakar, Wear, 248 (2001), 112–120